Developmental Cell, Vol. 5, 559–570, October, 2003, Copyright ©2003 by Cell Press

Phospholipid Membrane Composition Affects EGF Receptor and Notch Signaling through Effects on Endocytosis during *Drosophila* Development

Ursula Weber,[1] Cagla Eroglu,[2] and Marek Mlodzik[1,*]
[1]Brookdale Department of Molecular, Cell, and Developmental Biology
Mount Sinai School of Medicine
New York, New York 10029
[2]Structural and Computational Biology Programme
European Molecular Biology Laboratory
Meyerhofstrasse 1
D-69117 Heidelberg
Germany

Summary

The role of phospholipids in the regulation of membrane trafficking and signaling is largely unknown. Phosphatidylcholine (PC) is a main component of the plasma membrane. Mutants in the *Drosophila* phosphocholine cytidylyltransferase 1 (CCT1), the rate-limiting enzyme in PC biosynthesis, show an altered phospholipid composition with reduced PC and increased phosphatidylinositol (PI) levels. Phenotypic features of *dCCT1* indicate that the enzyme is not required for cell survival, but serves a role in endocytic regulation. *CCT1*$^-$ cells show an increase in endocytosis and enlarged endosomal compartments, whereas lysosomal delivery is unchanged. As a consequence, an increase in endocytic localization of EGF receptor (Egfr) and Notch is observed, and this correlates with a reduction in signaling strength and leads to patterning defects. A further link between PC/PI content, endocytosis, and signaling is supported by genetic interactions of *dCCT1* with *Egfr*, *Notch*, and genes affecting endosomal traffic.

Introduction

The biochemical and molecular aspects of signaling mechanisms are becoming quite well understood, but little is known about the cell biological aspects of the control of signaling except that receptor/ligand localization and trafficking are important features of the regulation (Entchev and Gonzalez-Gaitan, 2002; Krämer, 2002; Seto et al., 2002). The activity of several signaling pathways is controlled through regulated processing, secretion, and trafficking, or trans-endocytosis of the respective receptors and ligands (Krämer and Phistry, 1996; Lee et al., 2001; Lloyd et al., 2002; Parks et al., 2000). These include receptor tyrosine kinases (RTK; e.g., the EGF receptor, Egfr), Wg/Frizzled signaling, Notch signaling, and others. For example, the activity range of Wg in the embryo is restricted by endocytosis and lysosomal degradation in cells posterior to the Wg-expressing stripe (Dubois et al., 2001). Egfr activity is controlled through regulated ligand secretion (Lee et al., 2001) and receptor endocytosis (Lloyd et al., 2002). Similarly, Notch signaling levels are controlled via processing and endocytosis of its ligand Dl and Notch itself (Krämer, 2000; Lai et al., 2001; Parks et al., 2000; Pavlopoulos et al., 2001; Shaye and Greenwald, 2002).

The proteins governing such regulation are often associated with specific subcellular compartments and include Shibire (Shi), Hrs (*H*epatocyte growth factor-*r*egulated tyrosine kinase *s*ubstrate), Hook (Hk), and Deep Orange (Dor), each thought to affect specific steps in the endo- and/or exocytic pathways (Krämer, 2002; Seto et al., 2002). Whereas *shi* is required for endocytosis at the membrane, in particular the pinching off of vesicles, *Hrs* regulates the transition from early to late endosomes/multivesicular bodies (MVB). Dor and Hk are involved in the MVB-lysosome transition. Thus, a signaling component can be regulated at multiple levels within a cell.

The role of membrane composition in these processes remains obscure with the exception of "membrane rafts," which are membrane domains rich in cholesterol and sphingolipids that are thought to be involved in clustering of receptors and membrane-bound ligands (e.g., Anderson and Jacobson, 2002; Kenworthy, 2002). Are there membrane lipid composition cues that affect endocytosis or trafficking? We have identified mutations in a *Drosophila* phosphocholine *c*ytidylyl*t*ransferase (CCT), the rate-limiting enzyme in phosphatidylcholine (PC) biosynthesis (Vance et al., 1980). In *CCT* mutants, the phospholipid membrane composition is changed, resulting in defects in cellular trafficking.

It has been suggested that PC biosynthesis may be regulated in response to lipid requirements of vesicular trafficking (Huijbregts et al., 2000). CCT mutants bypass the Sec14p requirement in yeast (McGee et al., 1994) and CCT binds to p115/TAP in rat liver cells (Feldman and Weinhold, 1998). Interestingly, Sec14p binds PC itself and phosphatidylinositol (PI) and regulates Golgi-derived vesicle transport (McGee et al., 1994). Similarly, p115 is involved in vesicle trafficking and possibly docking of ER to Golgi vesicles (Shorter et al., 2002). These observations suggest that phospholipid metabolism and protein traffic are coordinated (Yanagisawa et al., 2002).

Here, we describe mutants in the *Drosophila CCT1* gene. Such mutants show an altered phospholipid composition, notably reduced PC levels, and a concomitant increase in PI. The phenotypic features of *CCT1* mutations argue for a role of this enzyme in endocytosis and membrane traffic. The subcellular localization of Egfr and Notch is affected in *CCT1* mutant cells. A link between *CCT1*, endocytosis, and signaling is further supported by genetic interactions of *CCT1* with Egfr and Notch signaling, and with genes affecting membrane trafficking.

Results

CCT1 Mutants Cause Specific Eye Phenotypes and Change the Phospholipid Composition

We have identified a semilethal P element insertion, *16919*, displaying a mild rough eye phenotype in homozygous escapers (not shown). Such eyes revealed de-

*Correspondence: marek.mlodzik@mssm.edu

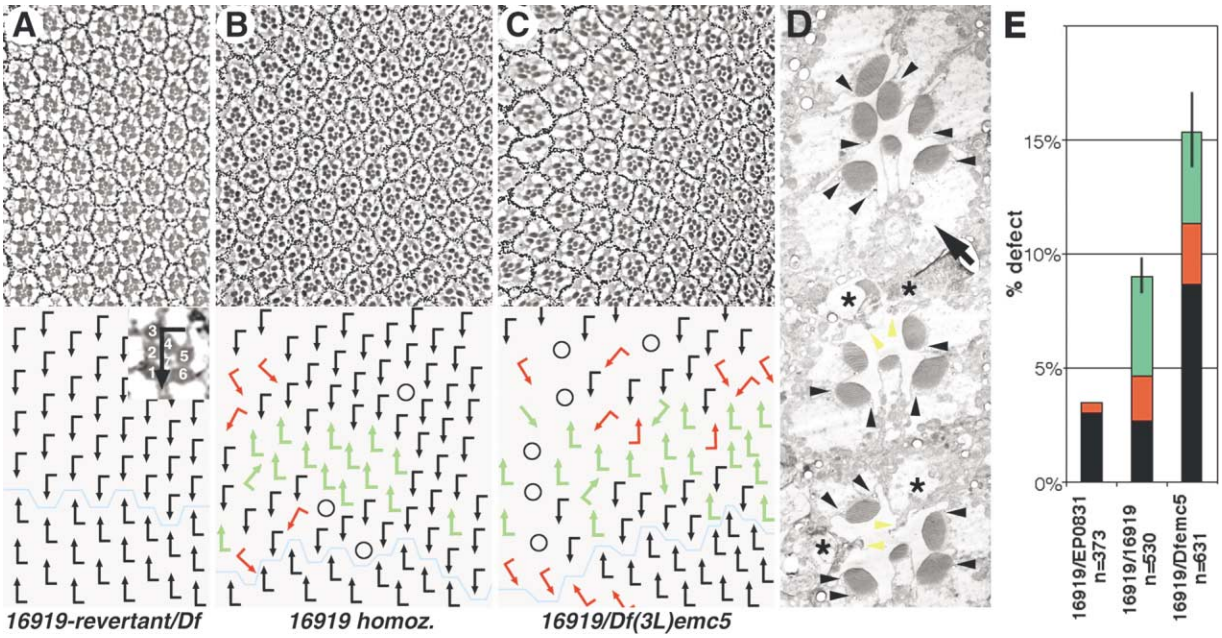

Figure 1. *CCT1* Mutants Have Defects in Eye Patterning and Terminal Photoreceptor Morphology

(A–D) Tangential adult eye sections around the dorsoventral midline, the equator, with schematic representation of ommatidial orientation. Anterior is left.

(A) *16919*-revertant-8/*Dfemc5* with wild-type (*wt*) pattern. The *16919* insertion phenotype (B and C) is revertible by P element excision. (B) *16919/16919*; (C) *16919/Df(3L)emc5*. Arrows in schematics are drawn as indicated in inset in (A); in *wt* (A), two chiral forms are opposed at the equator forming a mirror image symmetry line (light blue in scheme). Black arrows, correct orientation; red, misrotated ommatidia; green, opposite chirality for respective eye field; green arrows without flag, symmetrical ommatidia; black circles, ommatidia with missing/malformed photoreceptors. Note irregular arrangement and occasional missing photoreceptors in the mutant ([B and C]; quantified in [E]). *16919/Df(3L)emc5* eyes are often smaller, mostly ventrally (see also Figure 5E).

(D) TEM micrograph of *CCT1* null mosaic ommatidia. Mutant cells lack pigment. A *wt* ommatidium is shown at the top (black arrow) with all photoreceptors containing pigment granules (at base of rhabdomeres, examples marked by arrowheads) and rhabdomeres projecting toward the center of the ommatidium. Lower two ommatidia are mosaic. Asterisks indicate mutant cells, containing only traces of rhabdomeres (yellow arrowheads).

(E) Quantification of eye phenotypes of *CCT1* alleles: photoreceptor loss (black bar), ommatidial rotation (red bar), and chirality (green bar) defects are shown. Increasing defects are observed in *16919/EP0831* (4%), *16919/16919* (9.3% ± 1.5%), and *16919/Df(3L)emc5* (12% ± 3.2%) hypomorphic eyes. N, number of ommatidia analyzed. Standard deviation is for total defects.

fects in ommatidial polarity (chirality defects and misrotations) and photoreceptor number (Figures 1B and 1E). Confirming the specificity of this phenotype, *16919/Df(3L)emc5* flies showed a similar, but more penetrant phenotype (Figures 1C and 1E). In addition, *16919* homozygous or *16919/Df(3L)emc5* escapers are female sterile and lay few or no eggs, respectively (further supported by Gupta and Schüpbach, 2003). These features suggested that the gene disrupted by *16919* is required for eye patterning and female fertility. Precise excisions of the P element insertion completely reverted these phenotypes to wild-type (Figure 1A), confirming that they were caused by the P element.

Analysis of sequences flanking the P element revealed that it has inserted in the first intron of the predicted CG1049 gene (Figure 2A), which encodes a CCT. Subsequently, we will refer to this gene as *Drosophila CCT1*. An additional P element insertion in the vicinity (as reported in Flybase; http://www.flybase.org), *EP0831*, is allelic to *CCT1*, with similar eye phenotypes in escapers heterozygous with $CCT1^{16919}$ (Figure 1E). To confirm that *16919* and *EP0831* affect *CCT1* function, we have rescued their phenotypic defects with a transgene that includes the *CCT1* transcription unit and breaks in the two flanking genes (Figure 2A; Experimental Procedures).

Drosophila CCT1 is highly homologous to fly *CCT2* and to CCT genes from other species ranging from yeast to human (Figure 2B). The second related gene in *Drosophila*, *CCT2*, is located immediately downstream of *CCT1* (Figure 2A). CCT catalyzes the formation of CDP-choline during PC biogenesis (Clement and Kent, 1999; McGee et al., 1994) and is rate limiting in this pathway (Vance et al., 1980). Thus, it was surprising to find specific phenotypes associated with *dCCT1*. To confirm that the *CCT1* mutations indeed affect PC biogenesis, we compared the membrane composition of wild-type and *CCT1* mutant larvae. Strikingly, PC levels were reduced in membrane preparations from $CCT1^{16919}$/*Df(3L)emc5* and $dCCT1^{EP0831}$/*Df(3L)emc5* animals, whereas an increase in PI levels was detected (Figures 2C and 2D). These data confirmed that *CCT1* is required for PC biogenesis and demonstrated that in *CCT1* mutants the ratio of PC, PI, and PE is changed.

$CCT1^{16919}$ is a P element insertion carrying *lacZ*, thus acting as a reporter for *CCT1* expression. We used it to monitor *CCT1* expression, which was suggestive of its expression being patterned (see Supplemental Figure

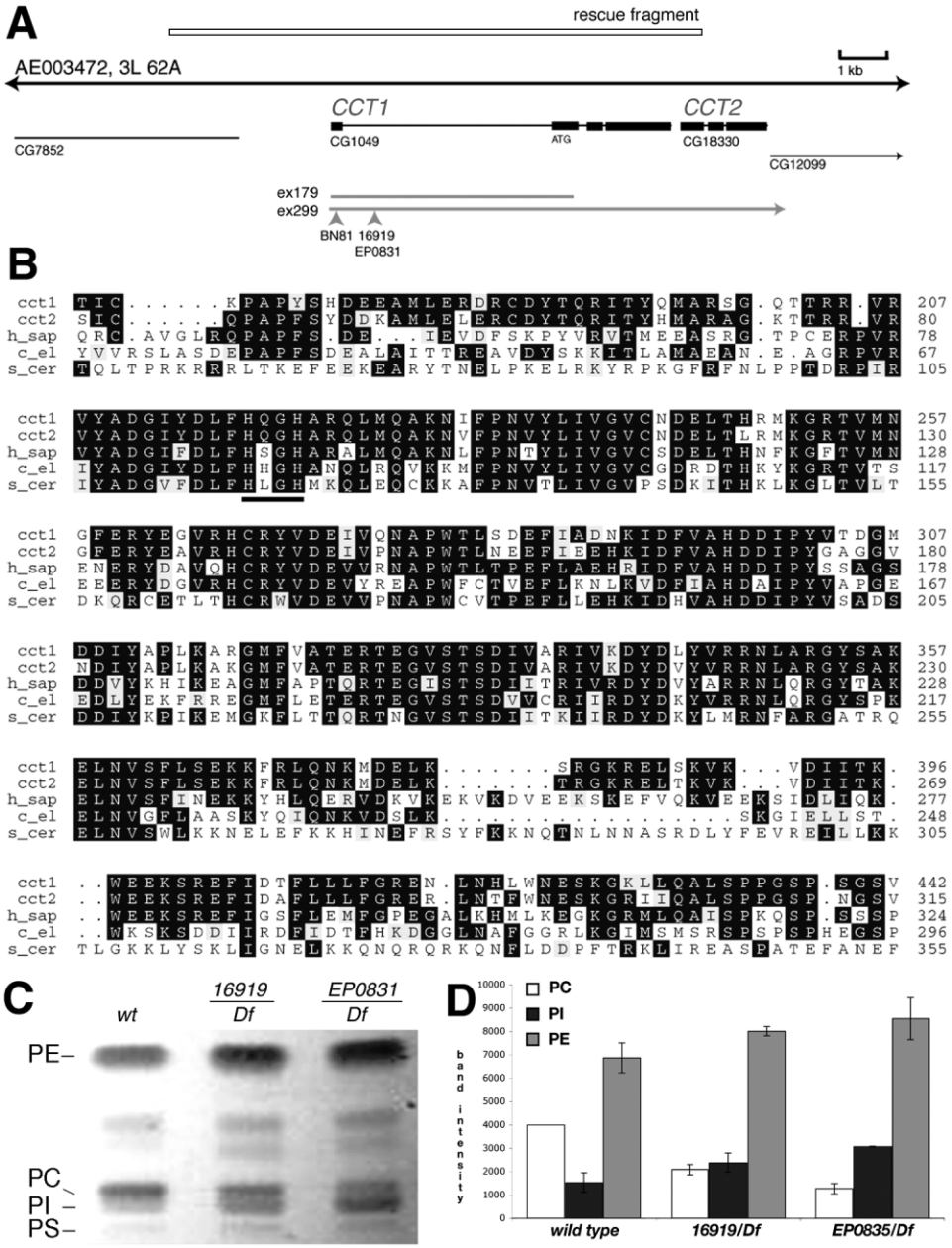

Figure 2. The *CCT1* Locus and Its Biochemical Function

(A) Genomic region of *CCT1* locus at 62A on chromosome 3L (according to Flybase). *16919* is inserted 170 bp upstream of *EP0831* at nucleotide 12236 of AC003472 (Flybase) in the first intron of *CCT1* (CG1049). *CCT1* alleles are indicated by gray arrowheads for P element insertions (hypomorphic alleles) and gray bars for excisions generated from P element BN81 (null alleles; Gupta and Schüpbach, 2003). The rescue construct is shown as an open bar above the map.

(B) Protein sequence alignment of the cytidylyltransferase domain of Dm CCT1 (Q9W0E0; SPTREMBL, http://srs.ebi.ac.uk), Dm CCT2 (Q9W0D9; SPTREMBL), and CCT of other species (*Homo sapiens* [h_sap] P49585, GenBank; *C. elegans* [c_el] P49583, GenBank; and *S. cerevisiae* [s_cer] P13259, GenBank). Identical residues are boxed in black, similar residues in gray. This *CCT1* domain shares 80% identity with fly *CCT2*, 61% with human *CCT*, 51% with *C. elegans CCT*, and 38% with yeast *CCT*. Alignment is shown from amino acid 166 to 442 of *dCCT1*. The HXGH motif is underlined.

(C and D) Phospholipid ratio of the plasma membrane is changed in *CCT1* mutants. PC levels are reduced in membrane preparations from $CCT1^{16919}$/*Df(3L)emc5* and $CCT1^{EP0831}$/*Df(3L)emc5* animals, whereas an increase in PI and PE is detected. PS is not affected. Position of phospholipid standards (PE, PC, PI, and PS) is indicated. Quantification in (D) shows the average of three experiments (*y* axis: arbitrary units).

S1 at http://www.developmentalcell.com/cgi/content/full/5/4/559/DC1; Gupta and Schüpbach, 2003). Interestingly, this pattern can be under the control of signaling input, in particular the Dpp and Egfr pathways (Supplemental Figure S1).

CCT1 Alleles Have Specific Eye Phenotypes

To determine the requirements of *CCT1* during cellular differentiation and development and because *CCT1* null mutants are lethal, we generated *CCT1* mutant tissue during eye development (Figures 1D and 3). Surprisingly,

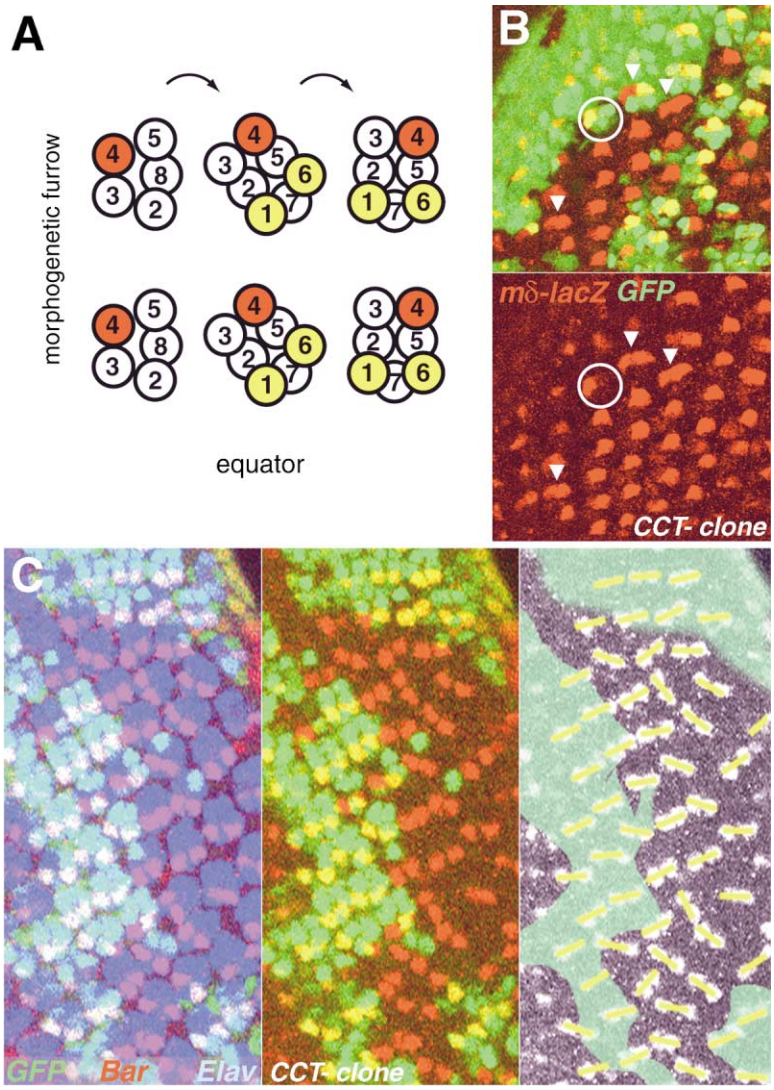

Figure 3. The *CCT1* Eye Imaginal Disc Phenotype Reveals Ommatidial Chirality and Rotation Defects

Dorsal fields of third larval instar eye discs are shown (anterior is left and dorsal is up).
(A) Cartoon highlighting the ommatidial rotation event; photoreceptors are indicated by numbers and R4 (*m*δ-*lacZ*, red) and R1/6 (Bar, yellow) marker expression.
(B and C) *CCT1* mutant tissue is marked by the absence of GFP (green).
(B) *CCT1*^{179} clone around ommatidial rows 3–8, where R3/R4 photoreceptor identity and ommatidial chirality are determined (MF is located in the left upper corner). *m*δ-*lacZ* (red) serves as R4 marker. Upper panel shows overlay; lower panel shows *m*δ-*lacZ*. Note several clusters with deregulated staining; often, both cells of the R3/R4 pair express *m*δ-*lacZ* (arrowheads) or show inverted *m*δ-*lacZ* expression in R3/R4 (circle). Such clusters reflect chirality defects in adult eyes (Figures 1A and 1B).
(C) *CCT1*^{16919} mosaic eye disc labeled with anti-Elav (blue; all photoreceptors) and anti-Bar (red; R1/R6, highlighting orientation of cluster). Right panel shows semischematic version of Bar staining (yellow bars) and the pale green approximately outlines wild-type tissue. Mutant or mosaic clusters are often misrotated. Both alleles shown here, *CCT1*^{16919} and *CCT1*^{179}, and *CCT1*^{299} gave similar results. Note that wild-type cells next to mutant areas can also show defects, suggesting a partial nonautonomy of these phenotypes.

CCT1^{-} cells initially develop normally with no obvious defects in cellular architecture (not shown) and give rise to tissue comparable in size to wild-type, indicating that *CCT1* is not required for cell growth or survival. *CCT1*$^{-}$ eye disc clones revealed patterning defects similar to those observed in adult eyes of the hypomorphic P alleles. Mutant ommatidial clusters often showed typical polarity defects (Figure 3B). Chirality defects are apparent using the (largely) R4-specific *m*δ-*lacZ* reporter (Cooper and Bray, 1999), which reflects cell fate selection in the R3/R4 pair and thus ommatidial chirality (Figure 3B). Mutant or mosaic clusters often showed aberrant *m*δ-*lacZ* expression, reflecting defects in Fz/Notch signaling in the R3/R4 pair. The photoreceptor R1/R6-specific marker Bar reveals the general orientation of developing ommatidial clusters and their degree of rotation (Figure 3C). In *CCT1* clones, many clusters have an aberrant orientation, displaying defects in ommatidial rotation (Figure 3C). These data suggest that *CCT1* can affect specific processes during eye development, in particular those related to planar cell polarization (PCP; Frizzled or Notch signaling; Cooper and Bray, 1999; Fanto and Mlodzik, 1999; Tomlinson and Struhl, 1999) and ommatidial rotation (Egfr signaling; K. Gaengel and M.M., submitted).

CCT1 is additionally required during terminal photoreceptor differentiation. Although *CCT1* null mutant photoreceptor cells initially appear normal, they do not form the light-harvesting organelle, the rhabdomere (Figure 1D). The rhabdomeres, containing the rhodopsin proteins, are large stacks of membrane microvilli that are formed at the apical membrane domain of each photoreceptor during their terminal differentiation (Izaddoost et al., 2002; Pellikka et al., 2002; Sang and Ready, 2002). Transmission electron microscopy (TEM) analysis of *CCT1* mutant photoreceptors revealed that the rhabdomeres failed to properly form (with only remnants of rhabdomeres sometimes to be found; Figure 1D). This defect is not light or age dependent (not shown) as is the case in many phototransduction mutants (Zuker, 1996), indicating that *CCT1* is autonomously required during the terminal differentiation of the rhabdomeric membrane stacks. Rhabdomere morphogenesis is thought to be a "burst" of apical membrane synthesis (Sang and

Ready, 2002), and it is also affected by blocking dynamin function (via photoreceptor-specific shi^{ts} expression (Acharya et al., 2003). Thus, this phenotype can be attributed to membrane trafficking defects (see below).

CCT1 Is Required during Egfr Signaling

The phenotypic features of *CCT1* during eye development suggested a requirement in one or several signaling pathways. Thus, we tested for genetic interactions between *CCT1* and components of most of the common signal transduction cascades. Strikingly, *CCT1* interacted with Egfr signaling. First, *CCT1* alleles dominantly suppressed the gain-of-function (GOF) *Ellipse* allele of *Egfr* (*Egfr^{ElpB1}*; Baker and Rubin, 1989). The *Egfr^{ElpB1}* phenotype is apparent in reduced eye size and loss of photoreceptors and ectopic veins in the wing. All aspects of the *Egfr^{ElpB1}* phenotype were suppressed by *CCT1* alleles (Figures 4A–4C). The degree and quality of suppression was comparable to that of loss-of-function (LOF) alleles of components of the Egfr/Ras pathway (Figures 4C and 4D, and not shown; Simon et al., 1991), suggesting a positive *CCT1* requirement in Egfr signaling. This observation was confirmed by the inverse interaction. The homozygous *CCT1^{16919}* eye phenotype is dominantly enhanced by *Egfr* (Supplemental Figure S2). The interactions between *CCT1* and *Egfr* are consistent with the *CCT1* eye phenotypes, as *Egfr* is required for photoreceptor induction, survival (Bergmann et al., 1998; Freeman, 1997; Kurada and White, 1998), and ommatidial rotation (K. Gaengel and M.M., submitted), suggesting that *CCT1* is required for Egfr signaling.

To corroborate this conclusion, we generated a catalytically inactive CCT1 by mutating two highly conserved His residues within the defining sequence element of a nucleotidyltransferase (HXGH, probably required for CTP binding; see Figure 2; Clement and Kent, 1999). The respective His-to-Ala mutations interfere with function, acting in a dominant-negative manner (Park et al., 1997). The CCT1[Ala] isoform, when expressed with *scalloped-Gal4* (Milan et al., 1997) in developing wings, causes ectopic wing venation defects (Figure 4D). This phenotype is enhanced by the removal of one copy of *Egfr*, showing an increasing effect with stronger alleles (Figure 4D).

Additional genetic evidence for a *CCT1* requirement in Egfr signaling comes from genetic interactions with *argos*, an inhibitory ligand of Egfr (Schweitzer et al., 1995). The sterility of homozygous *CCT1^{16919}* escapers is partially rescued by *aos* heterozygosity, and *aos* dominantly enhances the *CCT1* trans-heterozygous eye phenotype (not shown). Taken together, these data suggest that *CCT1* plays a positive role in Egfr signaling in the eye, wing, and probably also oogenesis.

CCT1 Is Positively Required for Notch Signaling

The ommatidial chirality defects in *CCT1* mutants suggested a role in PCP establishment, which is governed by an interplay of Fz-Notch signaling (Cooper and Bray, 1999; Fanto and Mlodzik, 1999; Tomlinson and Struhl, 1999). This was supported by our observation that *CCT1* alleles suppressed the PCP GOF phenotypes of *sev-Fz* and *sev-Dsh* (not shown), which display PCP defects with chirality inversions and symmetrical clusters (Boutros et al., 1998; Tomlinson et al., 1997). *CCT1* dominantly suppressed these aspects in both backgrounds, with many more ommatidia displaying a chiral arrangement (not shown). As PCP GOF eye phenotypes are modified by components of Fz or Notch pathways (Fanto and Mlodzik, 1999; Tomlinson and Struhl, 1999), we addressed this further and tested for an interaction between *CCT1* and *Notch* signaling in general.

Notch is haploinsufficient, showing a dominant LOF phenotype in strong alleles in the notching of the wing margin. Genetic modifications of this phenotype have been generally used to dissect the requirements of other genes in the context of Notch signaling (Gorman and Girton, 1992). In the *N* null allele, *N^{55e11}*/+, the wing notching phenotype is enhanced by removing one copy of *CCT1*, both with respect to the extent and frequency of the notch (Figures 5A and 5C).

In addition, although *N^{55e11}*/+ flies have no dominant eye phenotype in a wild-type background (Figure 5I), the simultaneous removal of one copy of *CCT1* and *aos* gives rise to rough eyes with many chirality defects (Figure 5D) and a partial loss of the ventral eye (Figure 5F). Such triple-heterozygous eyes resemble the stronger *CCT1^{16919}/Df(emc5)* phenotype (Figure 5E). Thus, although neither *N* nor *Egfr* signaling show dominant LOF eye phenotypes, the simultaneous removal of one copy of *CCT1* results in a haploinsufficiency of this genotype (Figure 5I). This not only supports a requirement for CCT1 in N signaling, but also suggests a link between *N* and *Egfr* signaling, possibly mediated through *CCT1*. Moreover, the homozygous *CCT1^{16919}* phenotype is strongly enhanced by a *Notch^{-}*/+ background, with severe wing notching (Figure 5B) and dramatically reduced eyes (Figure 5G) in rare escapers. These observations support the notion that *CCT1* is required for Notch signaling in several developmental contexts.

In summary, the above interactions suggest that *CCT1* function is critical for multiple signaling pathways. The phenotypic features and genetic interactions of *CCT1* argue for a role in (1) Egfr signaling (rotation), and (2) Notch signaling (chirality in eye and notching/size in the wing). Taken together with the biochemical role of CCT1, we suggest that the phospholipid composition of the membrane has an influence on the regulation of some signaling components, possibly mediated through membrane trafficking (see below).

CCT1 Mutant Cells Show an Increased Endocytic Activity and Have Enlarged Endosomes

As PC biosynthesis may be coupled to vesicular trafficking through an interaction between CCT and Sec14p and p115 (see Introduction), we wished to determine the primary defects in *CCT1* mutants and whether *CCT1* affects membrane traffic and endocytic pathways.

We made use of the fact that null mutant *CCT1* animals survive to the first larval instar stage, probably due to maternal contribution (Gupta and Schüpbach, 2003), and isolated their Garland cells, which are widely used to investigate endosomal trafficking and endocytosis (Kosaka and Ikeda, 1983; Lloyd et al., 2002; Sevrioukov et al., 1999). First instar larval Garland cells are seven times larger than imaginal disc cells and thus allow a detailed analysis of these cellular events. We cultured

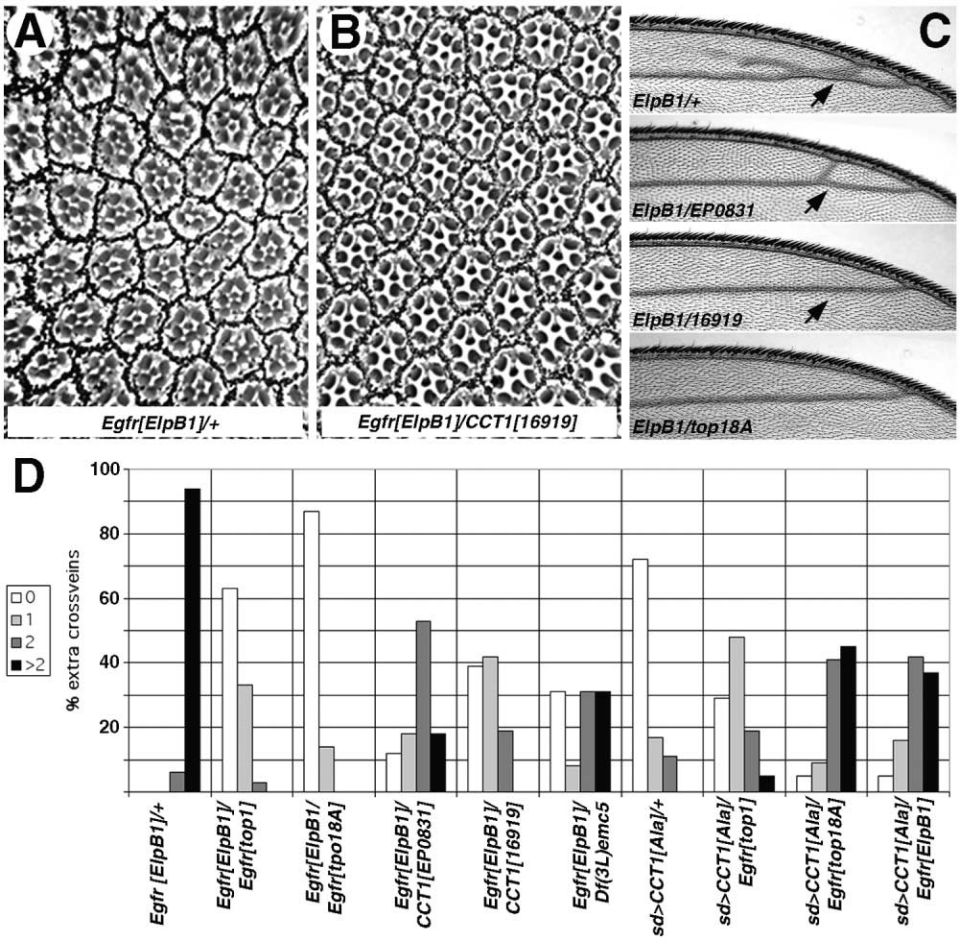

Figure 4. *CCT1* Is Required for Egfr Signaling

Genetic interactions between the GOF $Egfr^{ElpB1}$ phenotype and *CCT1*.

(A and B) Tangential eye sections of $Egfr^{ElpB1}/+$ (A) and $Egfr^{ElpB1}/+$, $CCT1^{16919}/+$ (B). Note regular arrangement and normal photoreceptor complement in (B). In $Egfr^{ElpB1}$ eyes, 77% (±7%) of ommatidia have a full complement of eight photoreceptors (A). This is rescued to 90% (±4%) by removing one copy of *CCT1* (B).

(C) Area of distal wings at the tip of vein L2; the following genotypes are shown from top to bottom: $Egfr^{ElpB1}/+$. $Egfr^{ElpB1}/+$, $CCT1^{EP0831}/+$. $Egfr^{ElpB1}/+$, $CCT1^{16919}/+$. $Egfr^{ElpB1}/+$, $Egfr^{top18A}/+$. The GOF allele $Egfr^{ElpB1}$ shows extra veins at the tip of L2 (first panel). *CCT1* mutations dominantly suppress this phenotype (middle panels), as do *Egfr* null alleles.

(D) Quantification of genetic interactions in the wing. Genotypes are indicated below the graph bars; the number of wings analyzed was between 13 and 35. Overexpression of a dominant-negative CCT form (CCT[Ala]) with *sd-Gal4* also causes extra veins at the tip of L2, which is dominantly enhanced by LOF and suppressed by GOF *Egfr* alleles.

the Garland cells, which are highly active excretory cells, in medium containing an endocytosis marker (Dextran red) and a lysosomal marker (Lysotracker). Subsequently they were analyzed with the endosomal compartment markers Hk, Dor, and Hrs (see Introduction).

Strikingly, both at the light microscopy level (determined by the number of Dextran red-uptaking vesicular puncta; Figures 6A, 6B, and 6I) and in TEM analysis (Figures 6E–6H and 6J), it was evident that $CCT1^{-}$ cells have an increased number of clathrin-coated pits (CCP) and vesicles (CCV). Whereas CCPs and CCVs are rare in wild-type Garland cells, they are abundant in $CCT1^{-}$ cells (Figures 6E, 6F, 6H, and 6J). Similarly, the endosomal compartment is enlarged as visualized with Rab7GFP, which labels the late endosome (Entchev and Gonzalez-Gaitan, 2002; not shown), and the number and size of MVBs are increased in *CCT1* mutants (Figures 6H and 6J). Colocalization of Dextran red and Lysotracker in $CCT1^{-}$ cells shows that traffic to the lysosome is not affected (Figures 6C and 6D). These data show that the primary defects in $CCT1^{-}$ cells are an increase in the rate of endocytosis, notably in the number of CCPs and CCVs, and a subsequent enlargement of the late endosome (Figure 6D). A *CCT1* role in endocytosis was confirmed by genetic interactions between CCT1 and mutations in genes regulating endocytosis, such as *hk*, *dor*, and *Hrs* (Supplemental Figure S2).

In summary, our comparison of wild-type and $CCT1^{-}$ Garland cells established that (1) endosomal trafficking to the lysosome is largely unchanged (Figures 6C and 6D), indicating that endocytic processing from vesicles through the early and late endosome to the lysosome

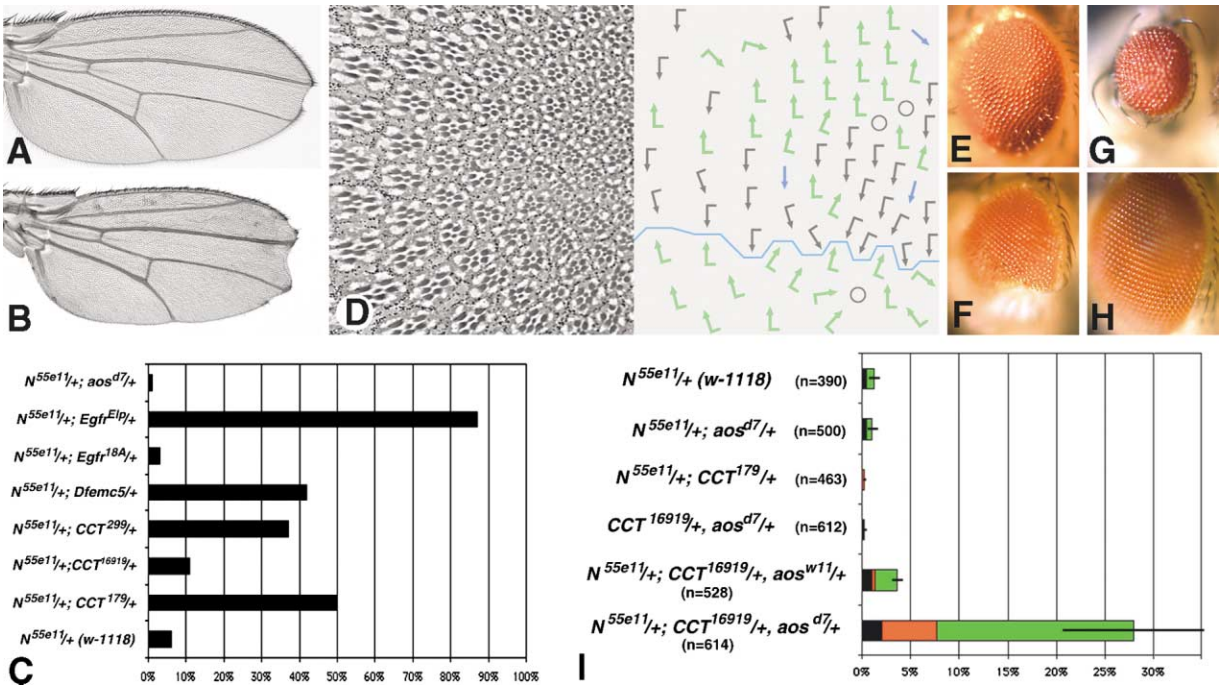

Figure 5. *CCT1* Mutants Enhance *Notch* Phenotypes

(A and B) The dominant wing phenotype (notches in the wing margin) of N^{55e11} allele is enhanced by *CCT1*. The wings of $Notch^{55e11}/+$ (A) and $Notch^{55e11}/+$; $CCT1^{16919/16919}$ (B) flies are shown. Notching is enhanced in size and frequency. Note also the reduction in wing size.

(C) Frequency of the distal notch phenotype, dominantly enhanced by *CCT1*/+. Note the stronger enhancement by null alleles as compared to $CCT1^{16919}$. $Egfr^{Elp}$ also enhances $Notch^{-}/+$.

(D and F) Heterozygous $N^{-}/+$; *CCT1*, *aos*−/+ combinations show a dominant eye phenotype.

(D) Tangential eye section around the equatorial region and corresponding schematic (right panel) of $N^{55e11}/+$; $CCT1^{16919}$, $aos^{d7}/+$ triple heterozygote eye. Black and green arrows represent the two chiral forms; blue arrows, symmetrical ommatidia; black circles, ommatidia with missing/supernumerary photoreceptors; blue line, equator. Clusters of ommatidia choose incorrect chirality, leading to fields of inverted ommatidia. Note the similarity to phenotypes in Figures 1B and 1C.

(E–H) External eye appearance of $CCT1^{16919}$/*Dfemc5* (E), $N^{55e11}/+$; $CCT1^{16919}$, $aos^{d7}/+$ (F), $N^{55e11}/+$; $CCT1^{16919/16919}$ (G), and *wt* eyes ([H], for comparison).

(I) Quantification of defects observed in heterozygous $N^{55e11}/+$ eyes. Color code and evaluation are as in Figure 1E.

is functioning, but that (2) endocytosis is significantly more active and thus the endosomal compartment is enlarged.

The Subcellular Localization of Egfr and Notch Is Altered in *CCT1* Mutant Tissue

Next, we analyzed the subcellular localization of Egfr and Notch and Hrs, Hk, Dor, Golgi, and ER markers in $CCT1^{-}$ imaginal disc cells (Figure 7, and not shown). In wild-type, Notch (Rand et al., 2000) and Egfr (Lesokhin et al., 1999) are detected at the apical membrane and in small punctae (vesicular structures) inside cells. Hrs is detected in a similar pattern and in early endosomal structures (Lloyd et al., 2002).

In $CCT1^{-}$ eye disc cells the punctate vesicular localization of Notch and Egfr was increased (with respect to the occurrence of these structures; Figure 7A). To assess trafficking of these receptors, we costained with the late endosomal marker Rab7GFP (Entchev and Gonzalez-Gaitan, 2002), which was expressed specifically in the R4 precursor (Figures 7B–7D). Rab7GFP colocalized with Notch and Egfr punctae in wild-type and $CCT1^{-}$ cells (Figures 7B–7D), showing that the receptors get processed to the late endosome in $CCT1^{-}$, like in wild-type cells. Similarly, Hrs and Egfr colocalized in the punctate structures in wild-type and $CCT1^{-}$ cells (yellow in Figures 7F and 7F′). Interestingly, Hrs and Notch displayed largely nonoverlapping expression patterns both in wild-type and $CCT1^{-}$ cells (Figures 7E and 7E′), consistent with Hrs labeling a subset of the endosomal compartment (not shown).

Taken together, these data suggested that (1) the vesicular endosomal structures containing Egfr and Notch are increased in number, and possibly size, in $CCT1^{-}$ cells, (2) the transport of the two receptors to the late endosome is not affected in $CCT1^{-}$ cells (as compared to wild-type), and (3) there are different subdomains within the endosomal structures (an Hrs-positive and an Hrs-negative one) to which Egfr and Notch differentially localize.

Discussion

Here we show that phosphocholine cytidylyltransferase *CCT1* mutants affect phospholipid membrane composition and membrane trafficking, causing an increase in

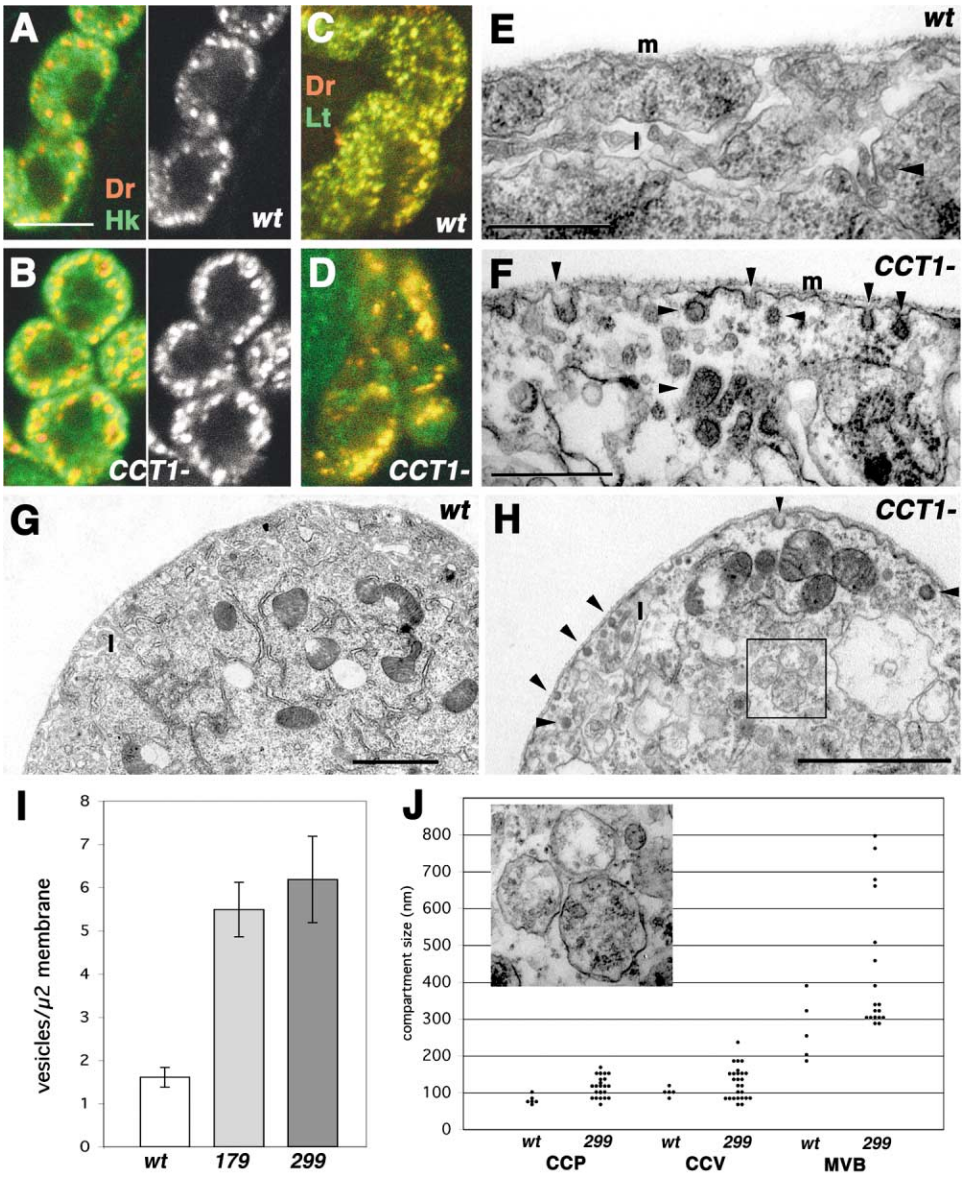

Figure 6. *CCT1*$^{-}$ Garland Cells Endocytose at a Higher Rate and Show Enlarged Endosomal Structures

Confocal (A–D) and TEM (E–H) images of *CCT1*^{299} and *wt* GCs (these cells are binucleated) and quantification (I and J) are shown.

(A and B) One minute Dextran red (DR) uptake and consecutive Hk staining (labeling endosome, in green) shows increased endocytosis in *CCT1*$^{-}$ (B) as compared to *wt* (A) GCs (quantified in [I]).

(C and D) Twenty minute Lysotracker (LT; green) uptake followed by 5 min DR (red) + LT. In wild-type (C), the small punctae are costained for DR and lysosomal marker (LT; green), appearing yellow.

(D) Five minute DR + LT uptake followed by 20 min LT shows enlarged late endosome and lysosome in *CCT1*$^{-}$ cells. Hk, Dor, and Hrs staining appeared increased in mutant cells ([B]; not shown).

(E–H) TEM analysis reveals that *CCT1*^{299} GCs have many more clathrin-coated pits and vesicles (CCP, CCV) and multivesicular bodies (MVB) but fewer labyrinthine channels (l); other compartments seem unaffected (m, basement membrane). Examples of CCPs and CCVs are marked by vertical and horizontal arrowheads, respectively, in (E)–(H); an area showing MVBs in (H) is boxed and shown at higher magnification as an inset in (J).

(I) Quantification of Dextran red vesicles based on confocal sections at the level of both nuclei of GCs. Three to nine cells from four individual animals (n = 172–639) were counted.

(J) Scatterplot showing individual size and number of CCPs, CCVs, and MVBs counted over the same membrane area in respective genotype as seen in TEM sections of six individual cells each. Both the number and size of each event is increased in *CCT1*$^{-}$ cells. Inset shows a cluster of MVBs (from [H]).

Scale bars represent 6 μ (A–D), 0.5 μ (E and F), and 2 μ (G and H).

endocytosis. This leads to signaling defects in at least two signaling pathways (Egfr and Notch) in some tissues, and to a failure in rhabdomere morphogenesis during terminal photoreceptor differentiation. The *CCT1* signaling phenotypes (and possibly also the rhabdomere differentiation defects) are likely due to the primary

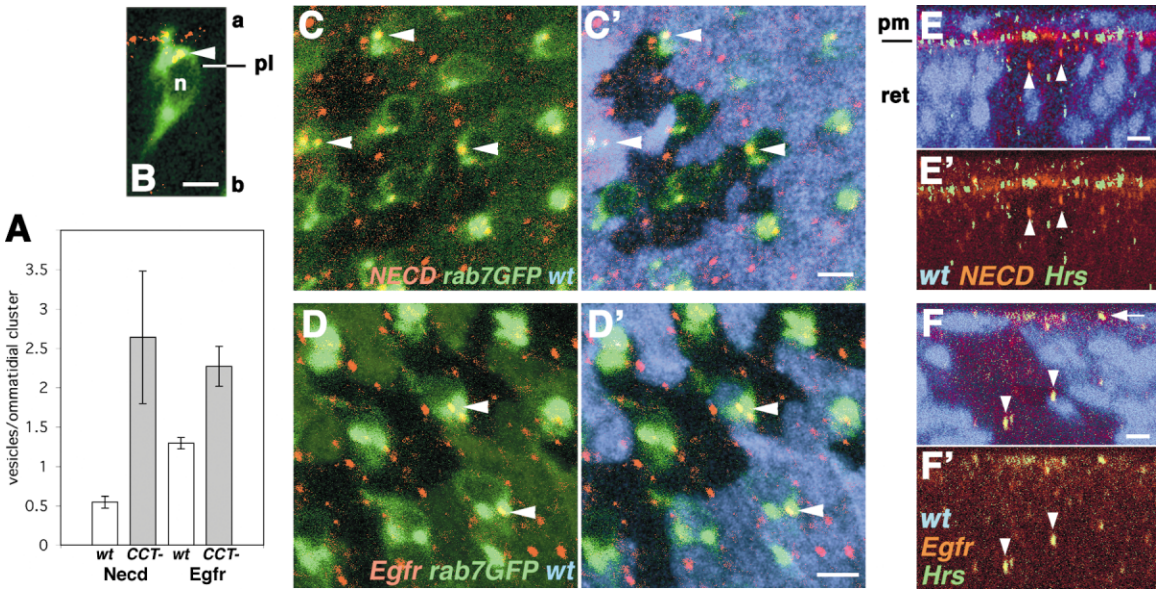

Figure 7. *CCT1* Affects the Subcellular Localization of N and Egfr

(A) Quantification of large vesicular punctae as seen with anti-Necd (Notch extracellular domain) and anti-Egfr stainings. The graph shows the frequency of such punctae per ommatidial cluster; white, wild-type; gray, *CCT1*$^{-}$. Quantification was assayed at five different optical section levels in XY sections at the level of nuclei. n = 116 for *N*, n = 146 for *Egfr* punctae.

(B–F) Confocal fluorescent microscopy sections of *CCT1*$^{-}$ clones in eye disc, around ommatidial rows 5–8 posterior to furrow. In (B)–(D), the Rab7GFP marker for the late endosome is driven by m∂-Gal4 in R4 precursors, highlighting strongly endosomal vesicles and cytoplasm weakly (green in [B], [C], [C′], [D], and [D′]). Anterior is left.

(B) XZ section through *CCT1*$^{-}$ R4 precursor stained with Rab7GFP (green) and anti-Necd (red). Note the overlap of anti-Necd with Rab7GFP (arrowhead); the bar (pl) marks the position of XY sections shown in (C) and (D); n, nucleus; a, apical; b, basal.

(C and C′) Mosaic eye disc stained as in (B). *wt* tissue is marked by β-gal (blue in [C′]; [C] shows red/green channel only). Note punctate colocalization (arrowheads) of Necd and Rab7GFP in both *wt* and *CCT1*$^{-}$ cells.

(D and D′) Mosaic eye disc stained with anti-Egfr (red) and Rab7GFP (green), and *wt* tissue marked by β-gal (blue in [D′]; [D] shows red/green only). Note colocalization (arrowheads) of Egfr and Rab7GFP. Both *CCT1*^{179} or *CCT1*^{299} null alleles show the same localization, indicating that endosomal trafficking and receptor downregulation function in mutant tissue as in *wt*. Rab7GFP expression had no phenotypic consequences as determined in eye sections. Anterior is left.

(E and E′) XZ section of mosaic disc stained with anti-Necd (red) and anti-Hrs (green), and *wt* tissue marked by GFP (blue; [E′] shows red/green only).

(F and F′) XZ section of similar *CCT1*$^{-}$ clone stained with anti-Egfr (red) and anti-Hrs (green), and *wt* tissue marked by GFP (blue; [F′] shows red/green only). Some large vesicular punctae are marked by arrowheads. Note that Egfr-positive punctae (red) costain for Hrs ([F and F′]; appearing yellow), and Notch and Hrs staining rarely coincides, suggesting that N and Egfr localize to distinct subdomains within the endosome. Hrs/Egfr or N-positive punctae (arrowheads) are larger in *CCT1*$^{-}$ cells and occur on average at 92.7 ± 2.9% (Hrs/Egfr) and 7.3± 2.9% (Egfr alone; n = 129) or at 77.6 ± 6.1% (Necd alone; n = 161) in *CCT1*^{179} (three discs each). Similar distribution is seen in *CCT1*^{16919}. The same applies for peripodial membrane (pm), indicated by arrow (ret, retina).

Scale bars represent 1 μ. Apical is up.

endocytosis defects. Our data suggest that a presumed "housekeeping" gene can specifically affect endocytosis and membrane trafficking.

Membrane Composition and Endocytosis

Cellular membrane and protein trafficking is a prerequisite for the complex functions cells need to perform during development and differentiation. Specific requirements for proteins in this context have been addressed in yeast (Schekman, 1992; Wendland et al., 1998) and complex multicellular organisms, such as *Drosophila* and nematodes (Krämer, 2000, 2002; Seto et al., 2002; Shaye and Greenwald, 2002). Although it has been proposed that membrane rafts play a role in receptor and ligand clustering (see Introduction), the role of membrane composition remains unclear.

CCT1^{-} cells have lower levels of PC and a simultaneous increase in PI and PE levels. Surprisingly, the CCT enzymes are not required for cellular survival, as even clones of the double null allele (*CCT*^{299}) show the same phenotypic features as the *CCT1*^{179} null, indicating that a cell can function with reduced PC and increased PI levels. This suggests that the alternate pathway of PE methylation can synthesize enough PC (Walkey et al., 1998) or that cells can function in many aspects with low PC levels. However, a decrease in PC (and an increase in PI) levels affects regulatory aspects of membrane dynamics and endocytosis. In addition, *CCT1* is the major gene responsible for the observed defects, as *CCT1*^{16919} and *CCT1*^{179} show the same phenotypes as the double null *CCT*^{299} allele.

The primary *CCT1* defect is an increase in the rate of endocytosis. In particular, more clathrin-coated pits (CCPs) and vesicles are observed, leading also to a size increase of the endosomal compartment. However, membrane traffic progression through the endosomal

compartment to the lysosome is not affected. This is in contrast to dynamin mutants (*shi*), where CCPs fail to pinch off and thus endocytosis is blocked (Kosaka and Ikeda, 1983).

An explanation for the increase of endocytosis in *CCT1* mutants might lie in the fact that decreased PC and increased PI levels affect the dynamics of the assembly and/or removal of the clathrin coat. PIP_2 (derived from PI) has been suggested to serve as a "docking site" for clathrin coat-promoting proteins, such as Epsin (Cadavid et al., 2000; Ford et al., 2002). It has been proposed that several factors, including dynamin, amphyphysin, and endophilin, can also initiate vesicle budding (Schmidt, 2002). An increase in PI and change in the PC/PI ratio is also interesting in the context of the proposal that Sec14p could monitor the PC/PI ratio and influence endocytosis (McGee et al., 1994). An alternative cause for the phenotypes observed might be the fact that the plasma membrane is normally asymmetric, with a difference in phospholipid composition between the outer and inner plasma membrane layers. Mammalian plasma membranes have higher PC content in the outer layer as compared to the inside face (Rothman and Lenard, 1977), suggesting that PC levels in the outer membrane layer serve a specific function.

CCT Regulation of Signaling Pathways

Cell surface receptor internalization and subsequent sorting to MVBs and lysosomal delivery are important mechanisms of signaling modulation (Lloyd et al., 2002; Seaman et al., 1996). Our analyses show that the phospholipid composition of the plasma membrane affects this process (Figure 6). The enlarged endosomal compartment is likely a consequence of the increase in endocytosis.

Genetic and histological analyses suggest that Egfr and N are sensitive to CCT1 function and possibly PC/PI levels. The Garland cell analysis and genetic interactions indicate that *CCT1*$^-$ cells have an increased rate of endocytosis, suggesting that plasma membrane (PM) proteins spend a shorter time at the PM with a reduced chance to interact with their ligands. As membrane trafficking to the lysosome is functioning in *CCT1*$^-$ cells, the overall levels of PM receptors might be reduced. Although the N and Egfr pathways are affected the most, it is likely that other receptors are also affected. Not all RTKs are equally sensitive to *CCT1* activity, however; for example, Sevenless (Sev) does not interact with *CCT1*. Furthermore, internalization of the Sev/Boss (Sev-ligand) complex is affected by *hk* mutants but is not manifest in an R7 loss phenotype (Krämer and Phistry, 1999). This suggests that signaling levels require tight regulation for some RTKs, such as Egfr, with multiple distinct responses at different signaling levels (Casci and Freeman, 1999; Freeman, 1997; Van Buskirk and Schüpbach, 1999), as compared to others such as Sev, with a simple on/off situation.

Both Egfr and N signaling levels are reduced in *CCT1* mutants, as deduced from the genetic interactions. The peak signaling levels for both pathways are affected in *CCT1*, whereas other aspects of their readout are less affected, supporting the notion that *CCT1* function is important for signaling level output in certain contexts only. Consistently for both pathways, regulated ligand and receptor processing and trafficking are critical for correct signaling levels (Dubois et al., 2001; Entchev and Gonzalez-Gaitan, 2002; Lee et al., 2001; Parks et al., 2000; Seto et al., 2002). Moreover, as *CCT1* expression can be regulated by signaling input (Supplemental Figure S1), a given cell population could regulate aspects of endocytosis through its membrane PC content.

It has recently been shown that a regulatory crosstalk between Egfr and Notch signaling is mediated through the transcriptional upregulation of a hypothetical factor by Egfr/Ras, leading to endocytosis and downregulation of Notch/LIN-12 in *C. elegans* (Shaye and Greenwald, 2002). Strikingly, we find that a heterozygous condition for both signaling pathways (that has no phenotypic consequence by itself) shows dramatic defects in a *CCT1*$^-$/+ background, also suggesting crosstalk between Egfr and Notch signaling. Thus, some aspects of the crosstalk between these and other pathways might be generally regulated or mediated through membrane phospholipid contents.

Experimental Procedures

Drosophila Stocks and Genetics

CCT1^{16919} was isolated in a screen for dominant suppressors of *sev-Jun[Asp]* (U.W., D. Bohmann, and M.M., unpublished data). The original chromosome was cleaned by recombination. *CCT1*^{16919} or *16919/Dfemc5* animals are semiviable and eclose with a few days' delay. *CCT1* null alleles 179 and 299 are lethal at first instar stage (kindly provided by T. Gupta and T. Schüpbach). *CCT1*^{EP0831} is third instar lethal over *Dfemc5* and was inserted at the same position as EP3346 (Flybase; obtained from Exelixis).

The following stocks were provided by individual labs: *aos*^{d5} by M. Freeman, *m*δ*-lacZ0.5* by F. Pichaud, *m*∂-Gal4 by K. Gaengel, *UAS-GFPrab7* by M. Gonzalez-Gaitan, and *w*^{a}, *N*^{55e11}/FM7c by E. Knust; *CCT1*$^-$, aos$^-$, and *sd-Gal4, UAS-CCT1[Ala]* were generated by recombination. All other stocks are from the Bloomington Stock Center. Crosses were performed at 25°C. *CCT1* clones were induced by the FLP/FRT system (Xu and Rubin, 1993) with *eyFLP* or *hsFLP* in *CCT1*$^-$ *FRT80B/ubiGFP FRT80B* or *arm-lacZ FRT80B* or *CCT1*$^-$ *FRT2A/ubiGFP FRT2A* flies. For *hsFLP*, one or two 1 hr heat shocks at 37°C were given on days 2 and 3 after egg laying.

Analysis of Phospholipids by Thin Layer Chromatography

Third instar larvae of *OreR* or *dCCT1*^{16919}*/Df(3L)emc5* and *dCCT*^{EP0831}*/Df(3L)emc5* genotypes were collected and their membranes were prepared (Rietveld et al., 1999) and phospholipids extracted as described (Bligh and Dyer, 1959), dried, and resuspended in 100 μl chloroform. Samples were normalized by phospholipid content, applied to an activated high-performance TLC plate (Merck), and developed with chloroform:methanol:water (65:25:4) as solvent. Phospholipids were visualized by iodine staining.

Histology and Antibody Stainings

Wing phenotypes were evaluated on the fly pad, mounted in Hoyers medium, and baked at 65°C overnight. For phenotypic evaluation of the eye, three out of six to eight sections were selected based on the strongest phenotype. Third instar eye discs were stained as described in *Drosophila* protocols (Sullivan et al., 2000). First instar larvae were collected at 17°C and their Garland cells cultured in Schneider's medium at 25°C, allowed to endocytose Dextran red at 300 μg/ml (Molecular Probes) and/or Lysotracker green at 3 μg/ml (Molecular Probes), washed in Schneider's medium at 4°C for 1 min, and then fixed and stained as eye discs. TEM: 90 nm sections of eyes or Garland cells were stained in 1:1 ethanol:aqueous saturated uranylacetate (5 min) and Reynold's lead citrate (3 min).

Antibodies used were rat-α-Elav and mouse-α-Necd from DSHB, rabbit-α-Bar (Higashijima et al., 1992), rabbit-α-β-gal (Cappel),

guinea pig-α-FL-Hrs (GP30; Lloyd et al., 2002), mouse-α-Egfr (Lesokhin et al., 1999), rabbit-α-Dor and rabbit-α-Hk (Sevrioukov et al., 1999), mouse-α-Golgi (Calbiochem), and αKDEL (ER marker; Stressgen). Confocal images were acquired on a Leica TCS. Stacks of optical sections spaced by 0.3 μ were projected for nuclear stainings in Figure 3 to represent each nucleus. Other confocal pictures are single sections.

Cloning and Transgenics

The rescue construct was a BamH1-Xho1 (nucleotides 8239–9430 of AC003472; Flybase) fragment subcloned into pW8 (Klemenz et al., 1987). One copy of this construct rescues the *EP0831/16919* or *16919/16919* eye phenotype and female sterility of *16919* and *16919/Dfemc5* mutant flies.

For CCT[Ala], His residues 218 and 221 were changed to alanine by PCR mutagenesis in EST Id12556, sequenced, and subcloned into pUAST. UAS-CCT1[wt] and UAS-CCT1[Ala] strains were established. DNA alignments were done with the GCG Wisconsin Package version 10.3.

Acknowledgments

We are grateful to T. Gupta and T. Schüpbach for sharing unpublished results and reagents. We thank N. Baker, H. Bellen, N. Colley, M. Freeman, H. Krämer, J. Culi, R. Mann, F. Pichaud, D. Ready, K. Saigo, A. Satoh, and the Bloomington Stock Center for fly strains and reagents, T. Weber, B. Winkler, and the Mlodzik lab for helpful discussions, C. Hu for generating transgenic flies, V. Williams for TEM experiments, and L. Giono for assistance. This work was supported by NIH grant GM62917 to M.M. and NIH-NCI shared resources grant R24 CA95823.

Received: January 31, 2003
Revised: June 10, 2003
Accepted: July 16, 2003
Published: October 6, 2003

References

Acharya, U., Patel, S., Koundakjian, E., Nagashima, K., Han, X., and Acharya, J. (2003). Modulating sphingolipid biosynthetic pathway rescues photoreceptor degeneration. Science *299*, 1740–1743.

Anderson, R.G., and Jacobson, K. (2002). A role for lipid shells in targeting proteins to caveolae, rafts, and other lipid domains. Science *296*, 1821–1825.

Baker, N., and Rubin, G.M. (1989). Effect on eye development of dominant mutations in *Drosophila* homologue of the EGF receptor. Nature *340*, 150–153.

Bergmann, A., Agapite, J., McCall, K., and Steller, H. (1998). The *Drosophila* gene hid is a direct molecular target of Ras-dependent survival signaling. Cell *95*, 331–341.

Bligh, E.G., and Dyer, W.J. (1959). A rapid method of total lipid extraction and purification. Can. J. Biochem. Physiol. *37*, 911–917.

Boutros, M., Paricio, N., Strutt, D.I., and Mlodzik, M. (1998). Dishevelled activates JNK and discriminates between JNK pathways in planar polarity and *wingless* signaling. Cell *94*, 109–118.

Cadavid, A.L.M., Ginzel, A., and Fischer, J.A. (2000). The function of the *Drosophila* fat facets deubiquitinating enzyme in limiting photoreceptor cell number is intimately associated with endocytosis. Development *127*, 1727–1736.

Casci, T., and Freeman, M. (1999). Control of EGF receptor signalling: lessons from fruitflies. Cancer Metastasis Rev. *18*, 181–201.

Clement, J.M., and Kent, C. (1999). CTP:phosphocholine cytidylyltransferase: insights into regulatory mechanisms and novel functions. Biochem. Biophys. Res. Commun. *257*, 643–650.

Cooper, M.T.D., and Bray, S.J. (1999). Frizzled regulation of Notch signalling polarizes cell fate in the *Drosophila* eye. Nature *397*, 526–529.

Dubois, L., Lecourtois, M., Alexandre, C., Hirst, E., and Vincent, J.P. (2001). Regulated endocytic routing modulates wingless signaling in *Drosophila* embryos. Cell *105*, 613–624.

Entchev, E.V., and Gonzalez-Gaitan, M.A. (2002). Morphogen gradient formation and vesicular trafficking. Traffic *3*, 98–109.

Fanto, M., and Mlodzik, M. (1999). Asymmetric Notch activation specifies photoreceptors R3 and R4 and planar polarity in the *Drosophila* eye. Nature *397*, 523–526.

Feldman, D.A., and Weinhold, P.A. (1998). Cytidylyltransferase-binding protein is identical to transcytosis-associated protein (TAP/p115) and enhances the lipid activation of cytidylyltransferase. J. Biol. Chem. *273*, 102–109.

Ford, M.G., Mills, I.G., Peter, B.J., Vallis, Y., Praefcke, G.J., Evans, P.R., and McMahon, H.T. (2002). Curvature of clathrin-coated pits driven by epsin. Nature *419*, 361–366.

Freeman, M. (1997). Cell determination strategies in the *Drosophila* eye. Development *124*, 261–270.

Gorman, M.J., and Girton, J.R. (1992). A genetic analysis of deltex and its interaction with the Notch locus in *Drosophila melanogaster*. Genetics *131*, 99–112.

Gupta, T., and Schüpbach, T. (2003). CCT1, a phosphatidylcholine biosynthesis enzyme, is required for *Drosophila* oogenesis and ovarian morphogenesis. Development, in press.

Higashijima, S., Kojima, T., Michiue, T., Ishimaru, S., Emorei, Y., and Saigo, K. (1992). Dual *Bar* homeo box genes of *Drosophila* required in two photoreceptor cells, R1 and R6, and primary pigment cells for normal eye development. Genes Dev. *4*, 1835–1847.

Huijbregts, R., Topalof, L., and Bankaitis, V. (2000). Lipid metabolism and regulation of membrane trafficking. Traffic *1*, 195–202.

Izaddoost, S., Nam, S.C., Bhat, M.A., Bellen, H.J., and Choi, K.W. (2002). *Drosophila* Crumbs is a positional cue in photoreceptor adherens junctions and rhabdomeres. Nature *416*, 178–183.

Kenworthy, A. (2002). Peering inside lipid rafts and caveolae. Trends Biochem. Sci. *27*, 435–437.

Klemenz, R., Weber, U., and Gehring, W.J. (1987). The white gene as a marker in a new P-element vector for gene transfer in *Drosophila*. Nucleic Acids Res. *15*, 3947–3959.

Kosaka, T., and Ikeda, K. (1983). Reversible blockage of membrane retrieval and endocytosis in the garland cell of the temperature-sensitive mutant of *Drosophila melanogaster*, shibirets1. J. Cell Biol. *97*, 499–507.

Krämer, H. (2000). RIPping notch apart: a new role for endocytosis in signal transduction? Sci. STKE *29*, 1–3.

Krämer, H. (2002). Sorting out signals in fly endosomes. Traffic *3*, 87–91.

Krämer, H., and Phistry, M. (1996). Mutations in the *Drosophila* hook gene inhibit endocytosis of the boss transmembrane ligand into multivesicular bodies. J. Cell Biol. *133*, 1205–1215.

Krämer, H., and Phistry, M. (1999). Genetic analysis of hook, a gene required for endocytic trafficking in *Drosophila*. Genetics *151*, 675–684.

Kurada, P., and White, K. (1998). Ras promotes cell survival in *Drosophila* by downregulating hid expression. Cell *95*, 319–329.

Lai, E.C., Deblandre, G.A., Kintner, C., and Rubin, G.M. (2001). *Drosophila* neuralized is a ubiquitin ligase that promotes the internalization and degradation of delta. Dev. Cell *1*, 783–794.

Lee, J.R., Urban, S., Garvey, C.F., and Freeman, M. (2001). Regulated intracellular ligand transport and proteolysis control EGF signal activation in *Drosophila*. Cell *107*, 161–171.

Lesokhin, A.M., Yu, S.Y., Katz, J., and Baker, N.E. (1999). Several levels of EGF receptor signaling during photoreceptor specification in wild-type, Ellipse, and null mutant *Drosophila*. Dev. Biol. *205*, 129–144.

Lloyd, T.E., Atkinson, R., Wu, M.N., Zhou, Y., Pennetta, G., and Bellen, H.J. (2002). Hrs regulates endosome membrane invagination and tyrosine kinase receptor signaling in *Drosophila*. Cell *108*, 261–269.

McGee, T., Skinner, H., Whitters, E., Henry, S., and Bankaitis, V. (1994). A phosphatidylinositol transfer protein controls the phosphatidylcholine content of yeast Golgi membranes. J. Cell Biol. *124*, 273–287.

Milan, M., Campuzano, S., and Garcia-Bellido, A. (1997). Developmental parameters of cell death in the wing disc of *Drosophila*. Proc. Natl. Acad. Sci. USA *94*, 5691–5696.

Park, Y.S., Gee, P., Sanker, S., Schurter, E.J., Zuiderweg, E.R., and Kent, C. (1997). Identification of functional conserved residues of CTP:glycerol-3-phosphate cytidylyltransferase. Role of histidines in the conserved HXGH in catalysis. J. Biol. Chem. *272*, 15161–15166.

Parks, A.L., Klueg, K.M., Stout, J.R., and Muskavitch, M.A. (2000). Ligand endocytosis drives receptor dissociation and activation in the Notch pathway. Development *127*, 1373–1385.

Pavlopoulos, E., Pitsouli, C., Klueg, K.M., Muskavitch, M.A., Moschonas, N.K., and Delidakis, C. (2001). neuralized encodes a peripheral membrane protein involved in delta signaling and endocytosis. Dev. Cell *1*, 807–816.

Pellikka, M., Tanentzapf, G., Pinto, M., Smith, C., McGlade, C.J., Ready, D.F., and Tepass, U. (2002). Crumbs, the *Drosophila* homologue of human CRB1/RP12, is essential for photoreceptor morphogenesis. Nature *416*, 143–149.

Rand, M.D., Grimm, L.M., Artavanis-Tsakonas, S., Patriub, V., Blacklow, S.C., Sklar, J., and Aster, J.C. (2000). Calcium depletion dissociates and activates heterodimeric notch receptors. Mol. Cell. Biol. *20*, 1825–1835.

Rietveld, A., Neutz, S., Simons, K., and Eaton, S. (1999). Association of sterol- and glycosylphosphatidylinositol-linked proteins with *Drosophila* raft lipid microdomains. J. Biol. Chem. *274*, 12049–12054.

Rothman, J., and Lenard, J. (1977). Membrane asymmetry. Science *195*, 743–753.

Sang, T.K., and Ready, D.F. (2002). Eyes closed, a *Drosophila* p47 homolog, is essential for photoreceptor morphogenesis. Development *129*, 143–154.

Schekman, R. (1992). Genetic and biochemical analysis of vesicular traffic in yeast. Curr. Opin. Cell Biol. *4*, 587–592.

Schmidt, A.A. (2002). The making of a vesicle. Nature *419*, 347–349.

Schweitzer, R., Howes, R., Smith, R., Shilo, B.Z., and Freeman, M. (1995). Inhibition of *Drosophila* EGF receptor activation by the secreted protein Argos. Nature *376*, 699–702.

Seaman, M.N., Burd, C.G., and Emr, S.D. (1996). Receptor signaling and the regulation of endocytic membrane transport. Curr. Opin. Cell Biol. *8*, 549–566.

Seto, E.S., Bellen, H.J., and Lloyd, T.E. (2002). When cell biology meets development: endocytic regulation of signaling pathways. Genes Dev. *16*, 1314–1336.

Sevrioukov, E.A., He, J.P., Moghrabi, N., Sunio, A., and Krämer, H. (1999). A role for the deep orange and carnation eye color genes in lysosomal delivery in *Drosophila*. Mol. Cell *4*, 479–486.

Shaye, D.D., and Greenwald, I. (2002). Endocytosis-mediated downregulation of LIN-12/Notch upon Ras activation in *Caenorhabditis elegans*. Nature *420*, 686–690.

Shorter, J., Beard, M.B., Seemann, J., Dirac-Svejstrup, A.B., and Warren, G. (2002). Sequential tethering of Golgins and catalysis of SNAREpin assembly by the vesicle-tethering protein p115. J. Cell Biol. *157*, 45–62.

Simon, M.A., Bowtell, D.D.L., Dodson, G.S., Laverty, T.R., and Rubin, G.M. (1991). Ras1 and a putative guanine nucleotide exchange factor perform crucial steps in the signaling by the sevenless protein tyrosine kinase. Cell *67*, 701–716.

Sullivan, W., Ashburner, M., and Hawley, R.S. (2000). *Drosophila* Protocols (Cold Spring Harbor, NY: Cold Spring Harbor Laboratory Press).

Tomlinson, A., and Struhl, G. (1999). Decoding vectorial information from a gradient: sequential roles of the receptors Frizzled and Notch in establishing planar polarity in the *Drosophila* eye. Development *126*, 5725–5738.

Tomlinson, A., Strapps, W.R., and Heemskerk, J. (1997). Linking Frizzled and Wnt signaling in *Drosophila* development. Development *124*, 4515–4521.

Van Buskirk, C., and Schüpbach, T. (1999). Versatility in signalling: multiple responses to EGF receptor activation during *Drosophila* oogenesis. Trends Cell Biol. *9*, 1–4.

Vance, D., Trip, E., and Paddon, H. (1980). Poliovirus increases phosphatidylcholine biosynthesis in HeLa cells by stimulation of the rate-limiting reaction catalyzed by CTP:phosphocholine cytidylyltransferase. J. Biol. Chem. *255*, 1064–1069.

Walkey, C., Yu, L., Agellon, L., and Vance, D. (1998). Biochemical and evolutionary significance of phospholipid methylation. J. Biol. Chem. *273*, 27043–27046.

Wendland, B., Emr, S.D., and Riezman, H. (1998). Protein traffic in the yeast endocytic and vacuolar protein sorting pathways. Curr. Opin. Cell Biol. *10*, 13–22.

Xu, T., and Rubin, G.M. (1993). Analysis of genetic mosaics in developing and adult *Drosophila* tissues. Development *117*, 1223–1237.

Yanagisawa, L.L., Marchena, J., Xie, Z., Li, X., Poon, P.P., Singer, R.A., Johnston, G.C., Randazzo, P.A., and Bankaitis, V.A. (2002). Activity of specific lipid-regulated ADP ribosylation factor-GTPase-activating proteins is required for Sec14p-dependent Golgi secretory function in yeast. Mol. Biol. Cell *13*, 2193–2206.

Zuker, C.S. (1996). The biology of vision of *Drosophila*. Proc. Natl. Acad. Sci. USA *93*, 571–576.

Note Added in Proof

The paper referred to as "K. Gaengel and M.M., submitted" is now in press: Gaengel, K., and Mlodzik, M. (2003). Egfr signaling regulates ommatidial rotation and cell motility in the *Drosophila* eye via MAPK/Pnt signaling and the Ras effector Canoe/AF-6. Development *130*, in press.